Response to Referee 1

Hong-Da Tai | egusphere-2026-1682

Dear Dr Tai,

Thank you for your careful assessment of the manuscript. Your comments identified four inconsistencies: in the physical interpretation of the environmental factor, the description of the correction coefficients, the comparison benchmark, and the reported regression uncertainties. Each has been corrected, and the conclusions have been revised to match. The multi-filter regression framework is retained. The revised manuscript distinguishes what the regressions show from the physical interpretation, which depends on the stated assumptions.

The annex reproduces Eqs. (1)–(13), the Appendix derivation and Tables 1–5 from the revised manuscript, so that the revisions discussed here can be checked in one place. Each item carries brief explanatory notes, and a final section summarises how Table 5 was reproduced. Manuscript numbering is retained. The annex belongs to this response; it is not a new manuscript supplement.

Your comments are reproduced below in italics. In my responses, equation, section, table and figure numbers refer to the revised manuscript. Numbers within the quoted comments refer to the original submission.

Comment 1 Interpretation of the environmental factor

Eq. (6) implies that background extinction can only lower the MOR measured outdoors, and the theoretical curve in Fig. 6, $f_{env} = 1/(1 + V_{cal}/V_{bg})$*, accordingly never exceeds 1. Table 4, however, gives* $f_{env} > 1$ *for PWD22 (1.161, 1.187) and SWS-200 Set B (1.077) and interprets these values as physical. By contrast, the SWS-200 Set E value (0.878), which is in the direction expected from Eq. (6), is described as not physically consistent with the additive-background interpretation (lines 380–382). In addition, the legend of Fig. 6 gives different values for the same four events (0.976, 1.023, 1.045 and 1.000), and the text quotes both sets: lines 289–290 describe the PWD22 values as "close to unity", while lines 359–360 quote 1.161 and 1.187. Could the author clarify the sign convention of* f_{env} *and which values are correct?*

Response

I agree with the referee. The original manuscript treated the regression-derived intercept factor as if it were a physical outdoor/darkroom MOR ratio. On that basis, it labelled factors above unity as physical and rejected the Set-E factor below unity. Neither classification is supported. The original model neglects indoor background extinction and therefore predicts an outdoor/darkroom MOR ratio no greater than one. Under that model, a factor above one cannot be interpreted as physical, and a factor below one gives no reason for rejection. Both classifications have been removed.

Definition and sign convention

$$\Delta C = C_{out} - C_{dark}, \qquad f_{env,reg} = exp(\Delta C).$$

The values in Table 4 are unchanged: 1.161 and 1.187 for PWD22 B01 Sets B and E, and 1.077 and 0.878 for SWS-200 B03 Sets B and E. The sign of ΔC indicates only whether the fitted outdoor intercept is higher or lower than the darkroom intercept. A factor above unity corresponds to a positive fitted intercept difference, and a factor below unity to a negative one. The sign alone does not show how much of that difference is caused by background extinction. The negative Set-E contrast is therefore not an error to be reversed.

Section 2.2 now states the reference convention $V_* = 1\ m$ explicitly. This makes the logarithms dimensionless while preserving the original numerical coefficients. It also fixes the meaning of the intercept factor: it is the ratio of the fitted responses at $1\ m$, which lies outside the tested reference-MOR range. When the outdoor and darkroom slopes differ, the fitted ratio within the measured range follows Eq. (6):

$$R_{fit}(V_r) = f_{env,reg} \cdot \left(\frac{V_r}{V_*}\right)^{a_{out} - a_{dark}}.$$

An intercept factor above unity therefore does not imply that the fitted outdoor response exceeds the fitted darkroom response across the measured range. A comparison with the physical model must use $R_{fit}(V_r)$, including the slope difference, and must take the model assumptions into account.

The table below illustrates this distinction numerically. It gives fitted outdoor/darkroom ratios at three reference MOR values: the lowest and highest filter-reference MOR listed in Table 2, and the geometric mean of all reference MOR values for each instrument and filter set. The geometric mean is computed from the logarithms of the reference values alone; it does not use LT31 measurements. The calculations retain the adopted sequences and use unrounded regression coefficients. Each approximate 95 % confidence interval applies only at the geometric-mean reference

MOR, under the stated regression assumptions. It does not describe the uncertainty at the lowest or highest reference MOR, nor does it form a confidence band across the whole filter range.

Sensor and set	Ratio at lowest reference	Geometric-mean reference MOR (m)	Ratio at geometric mean	Approx. 95 % CI at geometric mean	Ratio at highest reference
PWD22 B01 B	1.002	957.83	0.961	0.928 to 0.995	0.919
PWD22 B01 E	1.047	1,130.24	1.012	0.973 to 1.054	0.979
SWS-200 B03 B	1.059	1,369.37	1.052	0.970 to 1.142	1.048
SWS-200 B03 E	0.989	1,267.67	1.025	0.961 to 1.095	1.055

For PWD22 B01 Set B, the fitted ratio at the geometric-mean reference is below unity, and its conditional pointwise interval excludes unity. This does not contradict Table 4. Table 4 evaluates the intercept contrast at the adopted 1 m reference, whereas this comparison evaluates the fitted ratio at approximately 958 m. Because the fitted slopes differ, the estimated ratio and its uncertainty change with reference MOR, and the two results are consistent. Neither result, on its own, identifies the physical cause of the indoor–outdoor difference.

Original Figure 6 markers

The four marker values in the original Fig. 6 were not the Table 4 intercept factors, and they should not have been presented as interchangeable with them. Reconstruction from the archived measurements indicates that they were individual-filter outdoor/darkroom mean ratios. No single consistent rounding rule, however, reproduces all four displayed values exactly, so I do not claim an exact reconstruction of every label. The markers and grey crosses have been removed. The revised Fig. 6 shows model curves only, and the earlier “close to unity” interpretation has been replaced.

Scope of the physical model

The negligible-indoor-background expression cannot produce a physical ratio above unity. Section 2.4 and the Appendix now derive a conditional finite-background extension to examine whether such a ratio is physically possible. Its MOR form is Eq. (13):

$$R_{phys} = \frac{(1+V_{cal}/V_{bg,dark})}{(1+V_{cal}/V_{bg,out})}.$$

The extension rests on three assumptions: unchanged hardware response, the same effective filter contribution, and additive effective extinction. Under these assumptions, the ratio can exceed unity when outdoor background extinction is smaller than indoor background extinction. No negative absolute extinction is required. The extension shows that such behaviour is possible; it does not show that background differences explain the measured intercept factors.

Section 5.2 now states a quantitative limitation of this extension. Suppose the laboratory ceiling indication is taken as a lower bound of $20{,}000\ m$ on the true indoor background MOR. The model then gives $R_{phys} \leq 1 + V_{cal}/(20{,}000\ m)$. Some fitted ratios exceed this bound. For PWD22 B01 Set E, the fitted ratio at the lowest reference MOR of 252 m is approximately 1.047, against a conditional upper bound of 1.0126. For SWS-200 B03 Set B, the corresponding ratio at 230 m is approximately 1.059, against a bound of 1.0115. Under the assumed indoor background constraint, the model therefore cannot reproduce these point estimates. The comparison has two limitations. The laboratory ceiling indication does not independently establish the true background extinction, and the fitted ratios carry uncertainty. A point estimate exceeding the bound does not, by itself, show that the model is invalid.

The revised manuscript no longer assumes that background interference was negligible throughout every outdoor filter sequence. Section 4.2 now shows that the recorded LT31 session means do not satisfy the 10× criterion across the full filter-reference range of any adopted session. A session mean also cannot show whether the criterion was met within each filter-measurement interval, particularly when LT31 readings reached the reporting ceiling. Background variation, filter placement and slope–intercept coupling therefore remain possible contributors.

Table 4 now includes uncertainty intervals. At the adopted $1\ m$ reference, all four intercept-contrast intervals include zero, as discussed under Comment 4. This result applies to the intercept contrasts at 1 m only. It does not establish the fitted responses are indistinguishable throughout the measured range, nor that environmental interference is absent.

Revisions: Sects. 2.2 and 2.4, Eqs. (3)–(6) and (11)–(13), Sect. 4.2, Table 4, Fig. 6, Sect. 5.2 and the Appendix. The Abstract, objectives and Conclusion now describe a conditional decomposition.

Revised Figure 6 for Comment 1

Figure 6 now shows conditional model curves only. The former event markers and grey crosses have been removed.

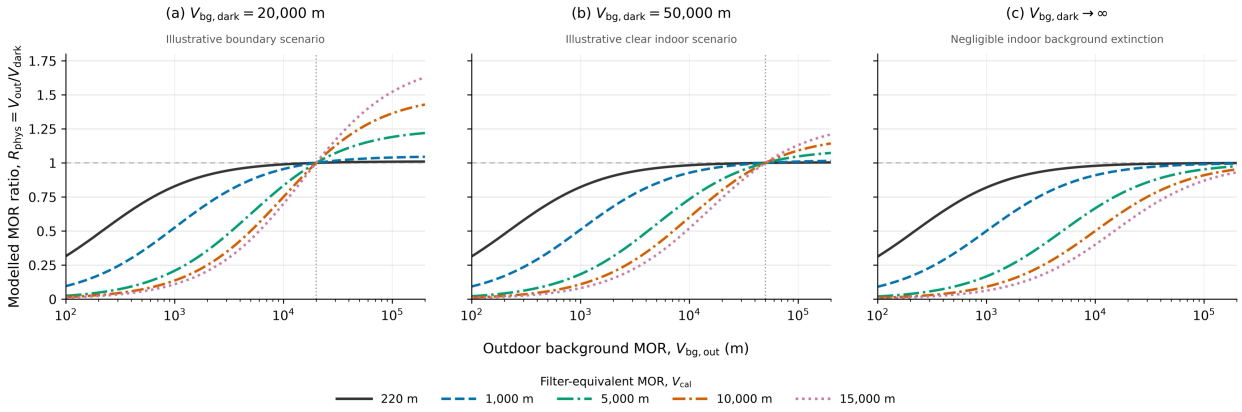


Figure 6: Modelled outdoor/darkroom MOR ratio under the conditional finite-background model. Panels show assumed indoor background MOR values of (a) 20,000 m, (b) 50,000 m, and (c) the negligible-indoor-background limit. Colours and line styles distinguish filter-equivalent MOR values of 220, 1,000, 5,000, 10,000, and 15,000 m. The horizontal dashed line denotes $R_{\mathbf{phys}} = 1$; vertical dotted lines in panels (a) and (b) mark equal indoor and outdoor background MOR, where all curves intersect unity. The finite indoor backgrounds are illustrative scenarios, not estimates of the laboratory conditions during the experiments. The curves assume unchanged hardware, an unchanged effective filter contribution and additive effective extinction. No experimental observations or regression-derived factors are plotted.

Comment 2 Coefficients used for the correction

According to Sect. 4.3.1 (lines 323–325), the PWD22 correction uses a_{ln} from the A01 darkroom regression (0.99 for Set B, as in the title of Fig. 8b) and C_{out} from the B01 outdoor sequence (0.125, Table 4). With these values, Eq. (5) gives $ln(V_{corrected}) = [ln(V_{meas}) - 0.125]/0.99$, which is smaller than $ln(V_{meas})$ everywhere in the observed MOR range. The Set-B correction should therefore lower all PWD22 values and make the global log-bias more negative, yet Table 5 and Fig. 8b show it changing from -0.010 to +0.020. Could the author check which parameter values were used for the Set-B correction?

Response

The referee is correct. The mixed coefficient combination described in the original text would lower the PWD22 values over the observed range. That description, however, did not match the implemented calculation, which used the slope and intercept from the same regression. Revised Table 3 identifies the source regressions, and Eq. (7) and Sects. 2.2 and 4.3.1 specify the procedure.

Sensor and set	Source regression	Slope	Intercept
PWD22 A01 B	A01 darkroom Sequence 1	0.993	−0.007
PWD22 A01 E	A01 darkroom Sequence 1	0.965	0.147
SWS-200 B03 B	B03 outdoor Sequence 1	0.995	0.017
SWS-200 B03 E	B03 outdoor Sequence 1	1.003	0.033

These are the coefficients used in the correction scripts. For PWD22 A01 Set B, Eq. (7) becomes:

$$ln\left(\frac{V^{out}_{corrected}}{V_*}\right) = \frac{ln(V^{out}_{uncorrected}/V_*)+0.007}{0.993}.$$

Subtracting the uncorrected logarithm gives:

$$\begin{aligned} ln\left(\frac{V^{out}_{corrected}}{V^{out}_{uncorrected}}\right) &= \ln\left(\frac{V^{\mathrm{out}}_{\mathrm{corrected}}}{V^*}\right) - \ln\left(\frac{V^{\mathrm{out}}_{\mathrm{uncorrected}}}{V^*}\right) \\ &= \frac{ln(V^{out}_{uncorrected}/V_*)+0.007}{0.993} - \ln\left(\frac{V^{\mathrm{out}}_{\mathrm{uncorrected}}}{V^*}\right) \\ &= \frac{ln(V^{out}_{uncorrected}/V_*)+0.007-0.993\cdot ln(V^{out}_{uncorrected}/V_*)}{0.993} \\ &= \frac{0.007\cdot ln(V^{out}_{uncorrected}/V_*)+0.007}{0.993} \end{aligned}$$

This change is positive over the observed MOR range, so the Set-B correction raises the PWD22 values rather than lowering them. Its magnitude on the Table 5 scale depends on the logarithmic base. Eq. (7) uses natural logarithms, whereas the field-comparison bias in Table 5 is the mean base-10 logarithm of the sensor-to-LT31 MOR ratio. The correction derived above is therefore divided by $\ln(10)$ when expressed on the residual scale of Table 5. Reproduction with the matched valid pairs confirms the increase in global log-bias. The global log_{10} bias is −0.009773 before correction and +0.020029 after Set-B correction, consistent with the rounded −0.010 and +0.020 in Table 5. The correction outputs and log-bias values are therefore retained; only the description of their provenance has been corrected. The benchmark percentages were recalculated separately, as explained under Comment 3.

The PWD22 A01 correction uses its own darkroom coefficients, not the B01 outdoor coefficients. A01 could not be tested outdoors with filters because it was committed to concurrent observations, so the B01 tests instead support the separate indoor–outdoor comparison in Table 4. B03 is treated differently. Its reported corrections use outdoor Sequence 1 coefficients for both filter sets, and the long-term observations in Fig. 9 and Table 5 were corrected with that slope and intercept. For B03 Set E, the indoor–outdoor contrast in Table 4 uses darkroom Sequence 2. The retrospective comparison retains the coefficients used in the original scripts. This choice does not establish that outdoor coefficients are generally preferable to darkroom coefficients. Neither time-series correction subtracts the Table 4 intercept contrast. These results therefore assess selected regression corrections; they do not independently validate the separation of hardware and environmental effects.

The revised manuscript also adds three qualifications. Applying the later calibration to the earlier deployment assumes that the instrument response remained sufficiently stable. The adopted A01 Set-E slope estimate changes the corrected MOR values, but its revised confidence interval includes one; it therefore does not establish a statistically significant departure from unit slope. The performance discussion now acknowledges that PWD22 absolute global log-bias and log-RMSE increase after correction, even though its benchmark agreement fraction increases.

Revisions: Eq. (7), Sects. 2.2 and 2.5, Sects. 4.3.1–4.3.4, Sects. 5.3–5.4, the Abstract and Conclusion.

Comment 3 Definition of the comparison benchmark

Sect. 1.1 (lines 32–33) notes that the WMO requirement is range-dependent: 50 m below 600 m, 10 % from 600 to 1500 m, and 20 % above 1500 m. The rest of the paper, however, uses a uniform ±10 % band labelled as the WMO tolerance (Fig. 2, the caption of Fig. 6, Figs. 8–9, Table 5, Sect. 5.4 and the Conclusions). This band is stricter than the WMO requirement over most of the range, in particular for the >10 000 m bin that dominates the residuals (lines 361–362), where the requirement is 20 %. It might help to describe the band as a simplified ±10 % benchmark, or to also report compliance against the range-dependent WMO requirement.

Response

I have adopted the referee's suggestion. The uniform band is now described as a study-defined ±10 % comparison benchmark and is not presented as WMO compliance. Section 3.4 defines it as $0.90 \leq V_{sensor}/V_{\mathrm{LT31}} \leq 1.10$, using the raw or corrected sensor MOR as appropriate. Section 1.1 keeps the range-dependent WMO guidance distinct from this benchmark, and the figures, captions, Table 5 and performance discussion have been updated accordingly.

Checking the implementation revealed a second discrepancy, between the original log-symmetric bounds and the intended percentage bounds. The original calculation used $|log_{10}(V_{sensor}/V_{\mathrm{LT31}})| \leq log_{10}(1.1)$, which corresponds to a ratio between 1/1.1 and 1.1. The revised calculation uses the stated ratio bounds of 0.90 and 1.10. The agreement fractions change as follows; the corrected observations and their log-bias and log-RMSE are unaffected:

Sensor	State	Original (%)	Revised (%)
PWD22 A01	Raw	16.7	17.9
PWD22 A01	Set B	22.4	24.5
PWD22 A01	Set E	37.1	39.2
SWS-200 B03	Raw	34.4	35.0
SWS-200 B03	Set B	27.4	27.9
SWS-200 B03	Set E	41.9	42.8

The ranking of correction states is unchanged. Set E increases the benchmark agreement fraction by 21.3 percentage points for A01 and 7.8 percentage points for B03. These percentages describe agreement among the sensor–LT31 pairs retained after the stated data exclusions; they do not measure compliance with a range-dependent operational standard. The 10 % background-contamination criterion in Sect. 2.4 is a separate modelling criterion and is identified as a practical benchmark.

Revisions: Sect. 3.4, figure labels and captions, Table 5, Sects. 4.3.2–4.3.4, Sect. 5.4 and the Conclusion; Sect. 2.4 clarifies the separate background criterion.

Revised Figure 2 for Comment 3

The revised annotations distinguish the illustration from a WMO compliance requirement.

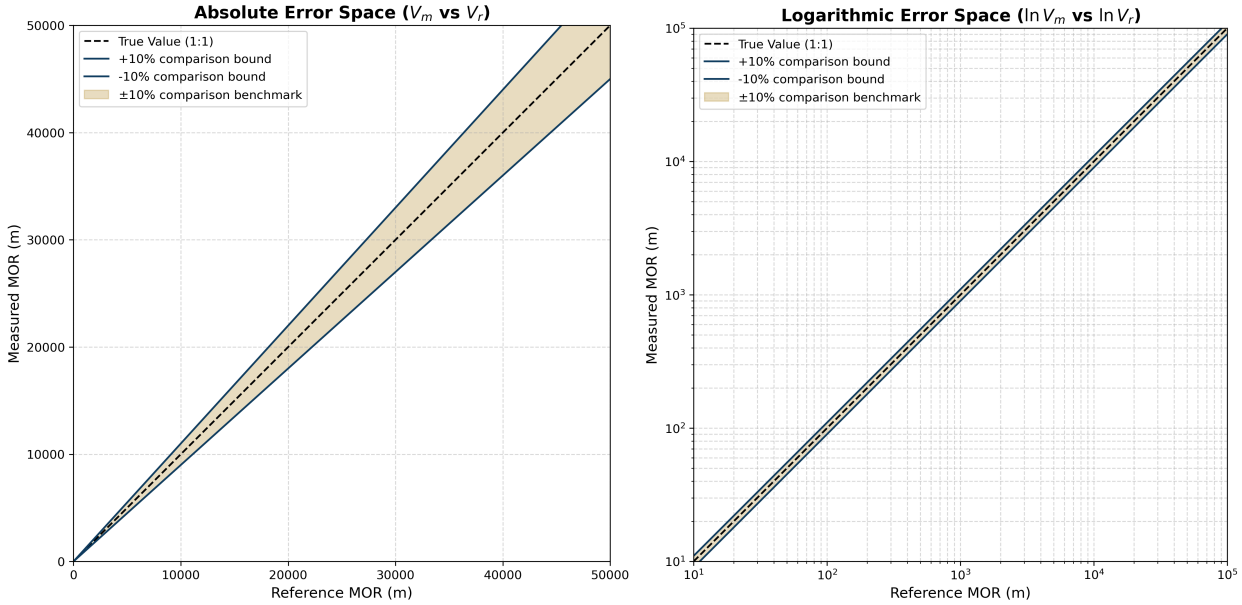


Figure 2: Comparison of measurement error structure in linear (left) and logarithmic domains (right). The multiplicative bias f appears as a constant proportional offset in linear space and as an additive shift in log-space, regardless of absolute MOR.

Revised Figure 8 for Comments 2 and 3

The correction results are unchanged. Benchmark labels, bounds and agreement percentages have been updated to match the revised definition and Table 5.

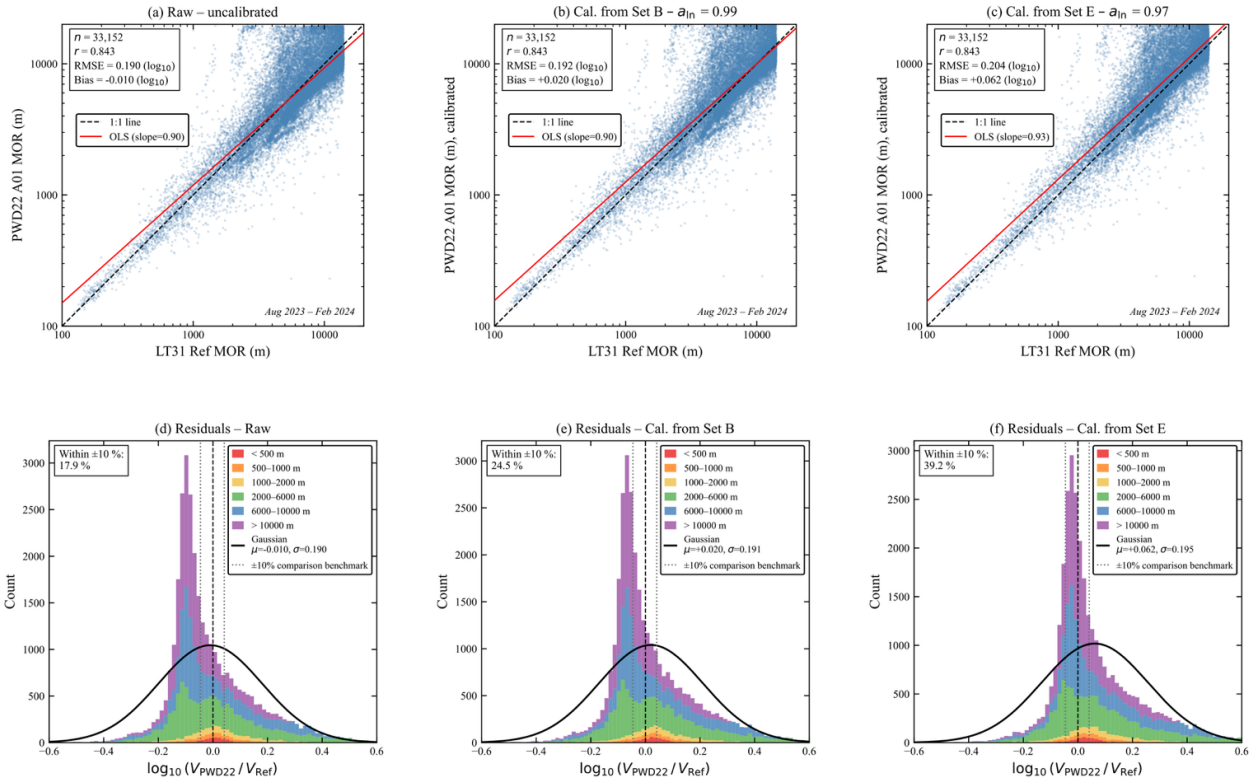


Figure 8: Top row: log–log scatter plots for (a) raw Vaisala PWD22 A01 (17 Aug 2023 – Feb 2024), (b) Set-B calibrated, and (c) Set-E calibrated MOR against LT31. Bottom row: histograms of $\log_{10}$(sensor MOR/LT31 MOR), using the uncorrected or corrected sensor MOR as appropriate, coloured by LT31 MOR bin, with fitted Gaussian envelopes. The dotted vertical lines at $\log_{10}(0.90)$ and $\log_{10}(1.10)$ delimit the ±10 % comparison benchmark; annotations give the percentage of retained pairs within these bounds.

Revised Figure 9 for Comments 2 and 3

The correction results are unchanged. Benchmark labels, bounds and agreement percentages have been updated to match the revised definition and Table 5.

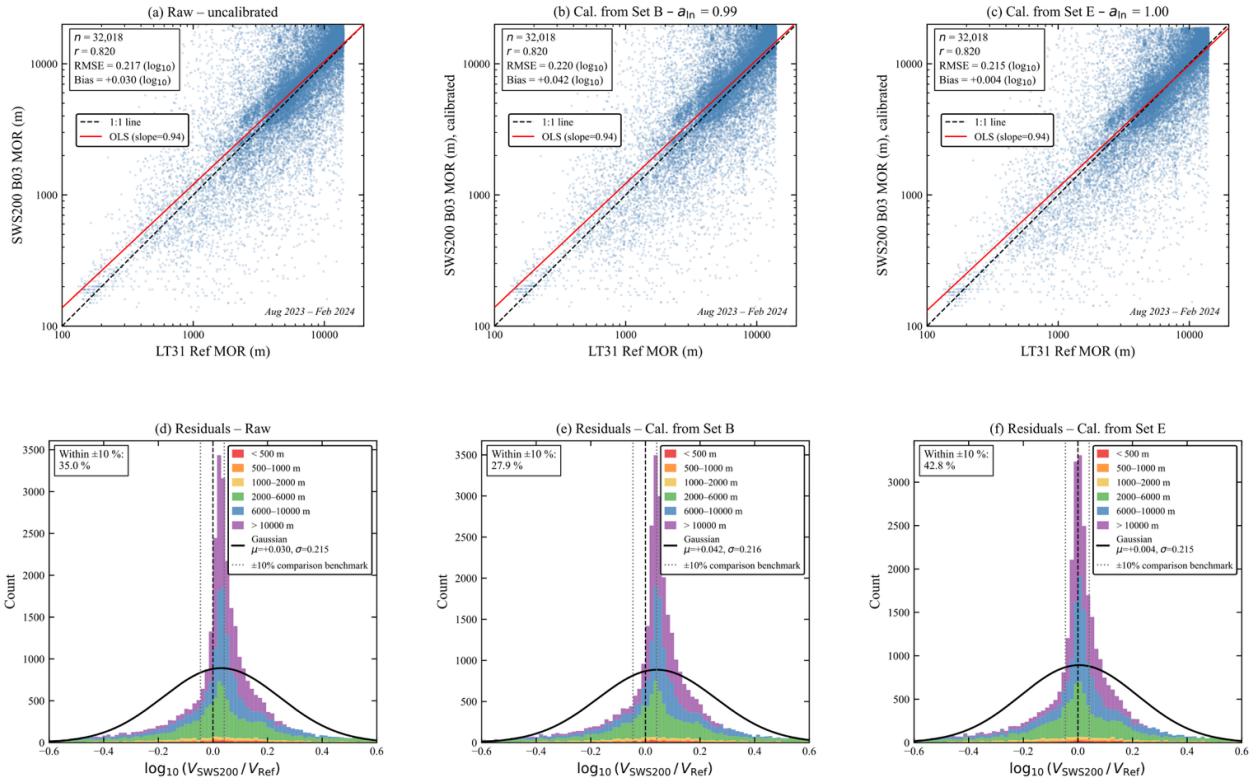


Figure 9: Top row: log–log scatter plots for (a) raw Biral SWS-200 B03 (17 Aug 2023 – Feb 2024), (b) Set-B calibrated, and (c) Set-E calibrated MOR against LT31. Bottom row: histograms of $\log_{10}$(sensor MOR/LT31 MOR), using the uncorrected or corrected sensor MOR as appropriate, coloured by LT31 MOR bin, with fitted Gaussian envelopes. The dotted vertical lines at $\log_{10}(0.90)$ and $\log_{10}(1.10)$ delimit the ±10 % comparison benchmark; annotations give the percentage of retained pairs within these bounds.

Comment 4 Regression uncertainties and their interpretation

In Table 3, the $CI_C(95\%)$ column appears to repeat the standard errors of the intercepts (e.g. -0.007 ± 0.014 with $CI_C = 0.014$). In contrast, $CI_{a_{ln}}$ is about t × SE (e.g. 0.002 → 0.006), and the legends of Fig. 5 also give intercept intervals of about t × SE (e.g. C = -0.01 ± 0.04 for A01 Set B Seq. 1). If so, the 95 % intercept intervals are about three times wider than listed, which would affect the statement in lines 269–270 and the uncertainty of $\ln(f_{env})$ obtained from Eq. (4).

Response

The referee is correct: the original intercept confidence-interval (*CI*) column repeated the standard errors, not the 95 % interval half-widths. Rechecking the calculation revealed a further error in my use of the regression output. The script applied an extra division by $\sqrt{s_{xx}}$, the square root of the sum of squared deviations of the regression's x-values from their mean, to a value already returned as a slope standard error. The intercept uncertainty and covariance propagation were also incorrect. The error lay in the analysis script, not in the regression module. The standard errors and approximate 95 % confidence-interval half-widths in Table 3 have been recalculated; the fitted point estimates are unchanged.

Section 4.1 now states the fitting convention explicitly. Ordinary least-squares regression was applied as $ln(V_r/V_*) = b \cdot ln(V_{meas}/V_*) + c$, and the coefficients were then transformed as $a_{ln} = 1/b$ and $C = -c/b$. First-order propagation includes the within-fit slope–intercept covariance. Table 3 reports each coefficient as estimate ± standard error and gives the approximate 95 % interval half-widths separately. The half-widths use Student-t critical values with $n - 2$ degrees of freedom: approximately 2.776 for the six-point PWD22 fits and 3.182 for the five-point SWS-200 fits.

The A01 darkroom Set-B Sequence 1 intercept illustrates the size of the correction. Its estimate is approximately −0.00670, with a corrected standard error of 0.03383 and a 95 % half-width of 0.09393. The revised Table 3 therefore reports −0.007 ± 0.034 and $CI_C = 0.094$. Two earlier inferences have been withdrawn as a result: the description of tightly constrained intercept uncertainties, and the treatment of agreement between the A01 and B01 darkroom intercepts as sufficient evidence for transferring calibration coefficients between units. Figure 5 and its caption now use the corrected approximate 95 % half-widths.

For Table 4, the propagated variances of the adopted indoor and outdoor intercepts are combined on the assumption that their fitted random errors are independent. Approximate intervals for ΔC use Welch–Satterthwaite effective degrees of freedom. The confidence limits for the factor are the exponentials of the lower and upper confidence limits for ΔC.

Sensor and set	ΔC	Approximate 95 % CI for ΔC	Approximate 95 % CI for factor
PWD22 B01 B	0.149	−0.093 to 0.391	0.912 to 1.478
PWD22 B01 E	0.171	−0.139 to 0.481	0.870 to 1.618
SWS-200 B03 B	0.074	−0.441 to 0.590	0.643 to 1.804
SWS-200 B03 E	−0.130	−0.582 to 0.322	0.559 to 1.380

Each interval is given as a lower limit followed by an upper limit. A contrast of zero corresponds to a factor of one, so the two columns express the same uncertainty on logarithmic and multiplicative scales.

All four contrast intervals include zero, and all four factor intervals include unity. As Sect. 4.2 now specifies, this statement concerns the intercept contrasts at $V_* = 1\ m$ only. It does not determine whether the fitted indoor and outdoor responses differ at other reference MOR values, where the slope difference also contributes. The intervals are also conditional on the regression model. The reference values are treated as fixed, uncertainty in both coordinates is not explicitly modelled, and shared reference uncertainty and other systematic contributions are excluded.

The revised discussion also separates Point CV (coefficient of variation) from regression uncertainty, because the two quantities describe different things. Point CV describes how the readings vary within each interval while the filter configuration remains unchanged. It does not measure the uncertainty of an intercept or reproducibility after remounting. Wider regression intervals indicate limited precision under the fitting model, but they do not diagnose a particular physical cause. All PWD22 darkroom slope intervals include unity. Overlapping intercept intervals are no longer used as evidence that coefficients are transferable between units.

Revisions: Sect. 4.1, Table 3 and caption, Fig. 5 and caption, Sect. 4.2, Table 4 and caption, Sect. 4.3.2, Sects. 5.1–5.3 and the Conclusion.

Revised Figure 5 for Comment 4

The regression annotations now report the recalculated approximate 95 % interval half-widths. Point error bars continue to describe within-interval variability.

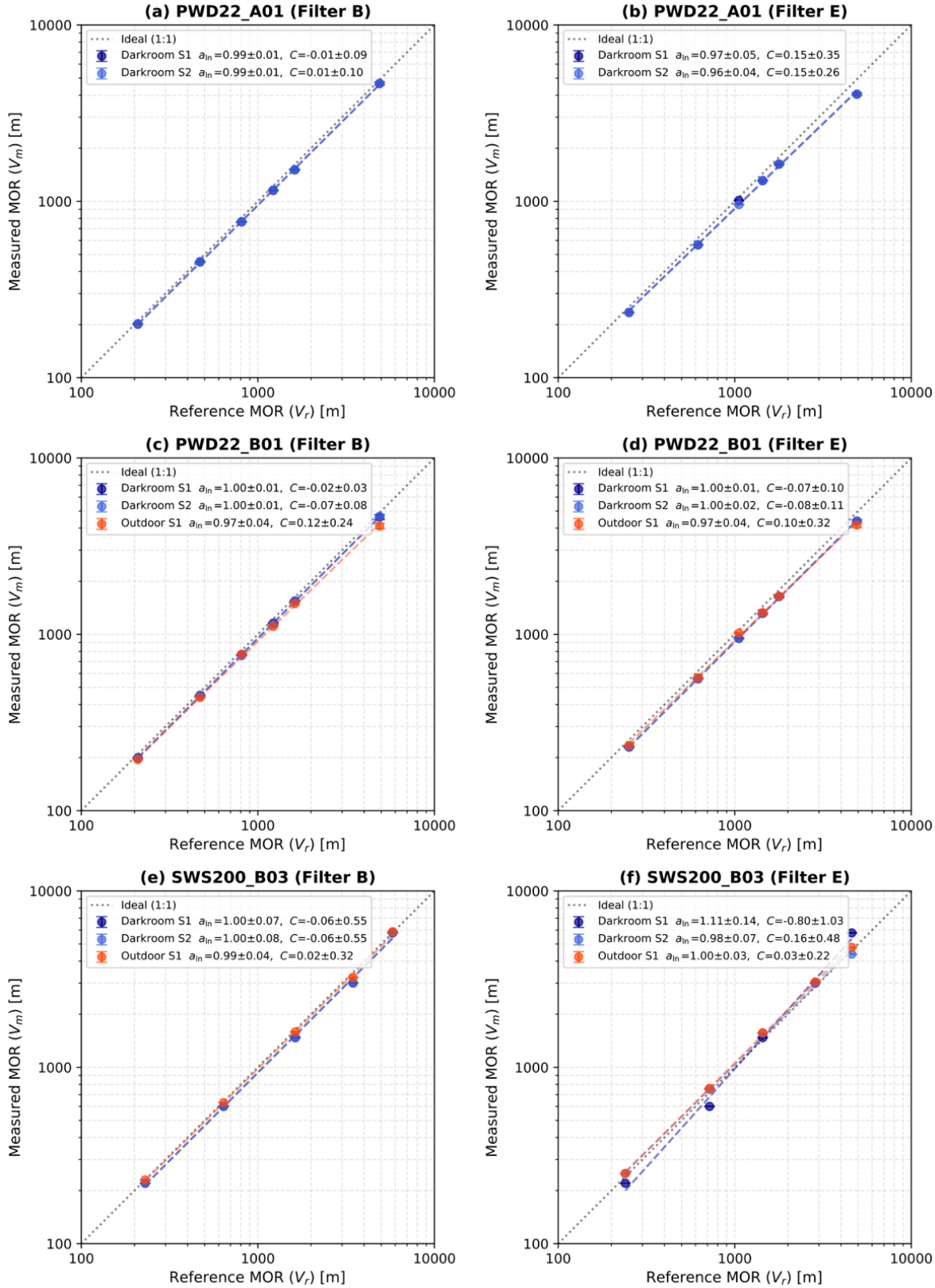


Figure 5: Six-panel comparison of darkroom and outdoor log-domain regressions for sensor units A01, B01, and B03 under filter sets B and E. Blue and red lines show the darkroom and outdoor regressions, respectively. Legend ± values are approximate 95 % confidence-interval half-widths under the adopted regression convention, with first-order propagation for the transformed coefficients; point error bars show within-interval standard deviations. The comparisons reveal differences in fitted slopes and intercepts, including sequence dependence, but do not independently identify their physical causes.

Related update to the LT31 background statistics

In revising the environmental interpretation, I also replaced the broad-window LT31 summaries with statistics matched to the selected filter-measurement intervals. The logger time zone was confirmed as KST (Korea Standard Time). Section 4.2 now specifies the procedure: the available one-minute readings are pooled across those intervals, intervening gaps are excluded, and the mean and sample standard deviation are reported.

Sensor and set	Original mean ± SD (m)	Revised mean ± SD (m)
PWD22 B01 B	15,000 ± 0	14,997 ± 47
PWD22 B01 E	13,281 ± 2,140	14,777 ± 717
SWS-200 B03 B	14,407 ± 2,057	10,740 ± 2,797
SWS-200 B03 E	14,975 ± 194	15,000 ± 0

These changes affect the description of the background during the filter tests, not the fitted intercept factors. The revised text also notes that the LT31 reporting ceiling is 15,000 m. A recorded mean of 15,000 m with zero SD therefore does not demonstrate a constant true atmospheric MOR.

I thank the referee again for identifying these issues. The empirical multi-filter comparisons and correction results are preserved. The uncertainty estimates have been corrected, the actual calculations are documented, and the physical claims are now limited to what the measurements support.

Sincerely,
Reno Kyu-Young Choi

Review annex to the response

This annex collects the equations and tables of the revised manuscript, so that the definitions, numerical changes and limits of interpretation can be assessed together. Tables 1 and 2 give the experimental context and reference assignments; Tables 3–5 give the revised statistical and performance results. The notes below are summaries; they make no additional claims of validation.

A1 Regression definitions and correction

Equation (1)

$$ln(V_{meas}) = a_{ln} \cdot ln(V_{ref}) + C$$

Equation (2)

$$C_{dark} = ln(f_{cal})$$

Equation (3)

$$f_{env,reg} = e^{(C_{out} - C_{dark})}$$

Equation (4)

$$C_{out} = C_{dark} + ln(f_{env,reg})$$

Equation (1) expresses the empirical log-linear response. Equation (2) identifies the indoor intercept with a hardware calibration term, but only if background interference is negligible and hardware and filter placement are reproducible. Equations (3) and (4) define the empirical intercept contrast. Equation (4) gives the difference between the fitted intercepts; it does not establish that this difference arises solely from atmospheric extinction.

Equation (5)

$$ln\left(\frac{V_j}{V_*}\right) = a_j ln\left(\frac{V_r}{V_*}\right) + C_j$$

Equation (6)

$$R_{fit}(V_r) = f_{env,reg}\left(\frac{V_r}{V_*}\right)^{a_{out} - a_{dark}}$$

Equation (7)

$$ln\left(\frac{V_{corrected}^{out}}{V_*}\right) = \frac{ln\left(\frac{V_{uncorrected}^{out}}{V_*}\right) - C_j}{a_j}$$

In Eqs. (5)–(7), $V_* = 1\ m$ preserves the original coefficient convention. In Eq. (6), the slope-difference term is essential: $\exp(\Delta C)$ is the fitted ratio at $1\ m$ and is not, in general, a constant ratio within the filter range. Equation (7) takes the slope and intercept from the same selected regression. A01 uses its own darkroom Sequence 1 coefficients; B03 uses outdoor Sequence 1 coefficients. The corrections evaluated in Table 5 apply Eq. (7) only; they do not additionally subtract the indoor–outdoor intercept difference, ΔC, reported in Table 4.

A2 Conditional effective extinction model

Equation (8)

$$\frac{1}{V_{meas}} = \frac{1}{V_{cal}} + \frac{1}{V_{bg}}$$

Equation (9)

$$\beta_{\mathrm{dark}} = \beta_{\mathrm{filter}} + \beta_{\mathrm{bg,dark}}$$

Equation (10)

$$\beta_{\mathrm{out}} = \beta_{\mathrm{filter}} + \beta_{\mathrm{bg,out}}$$

Equation (11)

$$R_{\mathrm{phys}} = \frac{V_{\mathrm{out}}}{V_{\mathrm{dark}}} = \frac{\beta_{\mathrm{filter}} + \beta_{\mathrm{bg,dark}}}{\beta_{\mathrm{filter}} + \beta_{\mathrm{bg,out}}}$$

Equation (12)

$$V_{bg} > 10 \times V_{cal}$$

Equation (13)

$$R_{\mathrm{phys}} = \frac{1 + V_{\mathrm{cal}}/V_{\mathrm{bg,dark}}}{1 + V_{\mathrm{cal}}/V_{\mathrm{bg,out}}}.$$

Equations (8)–(11) assume additive effective extinction and an unchanged effective filter contribution. This is a response model, not a general consequence of inserting an ND filter. In the negligible-indoor-background limit, $V_{dark} \approx V_{cal}$, and Eq. (13) reduces to $R_{phys} = 1/\left(1 + V_{cal}/V_{bg,out}\right)$. Equation (13) is Eq. (11) expressed in MOR and is the expression used in revised Fig. 6.

The finite-background ratio may be below, equal to or above unity while all absolute extinction contributions remain non-negative. Its equivalence to the empirical intercept factor is not established. Equation (12) bounds the background contribution relative to the filter contribution. It does not make that contribution constant across filter levels, nor does it establish negligible indoor background. The recorded session means do not show that this criterion was met at every filter level.

A3 Derivation reproduced from the manuscript Appendix

Definitions and common MOR conversion

$$K = -\ln(0.05),$$

$$V = \frac{K}{\beta}.$$

$$V_{\mathrm{cal}} = \frac{K}{\beta_{\mathrm{filter}}},$$

$$V_{\mathrm{bg,dark}} = \frac{K}{\beta_{\mathrm{bg,dark}}},\ V_{\mathrm{bg,out}} = \frac{K}{\beta_{\mathrm{bg,out}}}.$$

Here, β denotes the extinction coefficient associated with V. In the filter model, it represents the assumed effective extinction, and V_{cal} is the filter-equivalent MOR assigned to each configuration, not the unfiltered laboratory background MOR. Zero background extinction corresponds to a background MOR tending to infinity.

Under the assumed additive effective-extinction model:

$$V_{\mathrm{dark}} = \frac{K}{\beta_{\mathrm{filter}} + \beta_{\mathrm{bg,dark}}},$$

$$V_{\mathrm{out}} = \frac{K}{\beta_{\mathrm{filter}} + \beta_{\mathrm{bg,out}}}.$$

Taking the outdoor/darkroom ratio:

$$\begin{aligned} R_{\mathrm{phys}} &= \frac{V_{\mathrm{out}}}{V_{\mathrm{dark}}} \\ &= \frac{\beta_{\mathrm{filter}} + \beta_{\mathrm{bg,dark}}}{\beta_{\mathrm{filter}} + \beta_{\mathrm{bg,out}}} \\ &= \frac{1 + \beta_{\mathrm{bg,dark}}/\beta_{\mathrm{filter}}}{1 + \beta_{\mathrm{bg,out}}/\beta_{\mathrm{filter}}} \\ &= \frac{1 + V_{\mathrm{cal}}/V_{\mathrm{bg,dark}}}{1 + V_{\mathrm{cal}}/V_{\mathrm{bg,out}}}. \end{aligned}$$

$$\ln(R_{\mathrm{phys}}) = \ln\left(1 + \frac{V_{\mathrm{cal}}}{V_{\mathrm{bg,dark}}}\right) - \ln\left(1 + \frac{V_{\mathrm{cal}}}{V_{\mathrm{bg,out}}}\right)$$

In the negligible-indoor-background limit under the stated model assumptions:

$$\begin{aligned} V_{\mathrm{bg,dark}} &\to \infty \\ R_{\mathrm{phys}} &= \frac{1}{1 + V_{\mathrm{cal}}/V_{\mathrm{bg,out}}} \\ \ln(R_{\mathrm{phys}}) &= -\ln\left(1 + \frac{V_{\mathrm{cal}}}{V_{\mathrm{bg,out}}}\right). \end{aligned}$$

$$R_{\mathrm{phys}} \leq 1$$

For finite indoor background, a ratio above unity requires:

$$R_{\mathrm{phys}} > 1 \Leftrightarrow \beta_{\mathrm{bg,out}} < \beta_{\mathrm{bg,dark}} \Leftrightarrow V_{\mathrm{bg,out}} > V_{\mathrm{bg,dark}}$$

No negative absolute extinction is required. The ratio generally depends on the filter-equivalent MOR and need not produce a constant intercept shift. The Appendix establishes conditional model behaviour, not a quantitative explanation of every measured ratio. As Section 5.2 explains, if the true indoor background MOR is at least 20,000 m, the model gives $R_{phys} \leq 1 + V_{cal}/(20{,}000\ m)$. Some fitted ratios, R_{fit}, exceed this upper bound, so the model cannot reproduce those point estimates under that assumption.

A4 Manuscript tables

Tables retain their manuscript numbers and numerical entries. Formatting is adapted to the response page.

Manuscript Table 1

Table 1: Decoupling dataset acquisition schedule.

Instrument Model	Filter Set	Test Environment	Acquisition Date
Vaisala PWD22 (A01)	Set B	Indoor (Darkroom)	19 & 23 July 2024
	Set E		18 & 23 July 2024
Vaisala PWD22 (B01)	Set B	Indoor (Darkroom)	7 & 8 August 2024
	Set E		9 August 2024
	Set B	Outdoor (Field)	4 & 5 September 2024
	Set E		6 & 7 September 2024
Biral SWS-200 (B03)	Set B	Indoor (Darkroom)	5 August 2024
	Set E		2 August 2024
	Set B	Outdoor (Field)	10 & 11 September 2024
	Set E		12 & 13 September 2024

Interpretation summary. The schedule separates the 2024 filter campaigns from the August 2023–February 2024 continuous comparison. Applying the calibration retrospectively assumes sufficiently stable instrument response. The schedule lists the campaigns; Table 4 identifies the adopted sequences.

Manuscript Table 2

Table 2: Multi-Filter Combination and Reference MORs

Instrument model	Filter combination					
	Set B			Set E		
	Transmitter	Receiver	Reference MOR ($\boldsymbol{V_r}$) [m]	Transmitter	Receiver	Reference MOR ($\boldsymbol{V_r}$) [m]
Vaisala PWD22	None	ND1.0	209	None	ND1.0	252
	ND0.5	ND1.0	471	ND0.5	ND1.0	620
	ND0.6 + ND0.3	ND1.0	810	ND0.6 + ND0.3	ND1.0	1,056
	ND1.0	ND1.0	1,222	ND1.0	ND1.0	1,440
	ND1.3	ND1.0	1,619	ND1.3	ND1.0	1,783
	ND2.0	ND1.0	4,895	ND2.0	ND1.0	4,921
Biral SWS-200	ND0.3	ND0.6	230	ND0.3	ND0.6	240
	ND0.3 + ND0.5	ND0.6	640	ND0.3 + ND0.5	ND0.6	720
	ND1.3	ND0.6	1,630	ND1.3	ND0.6	1,440
	ND1.3 + ND0.4	ND0.6	3,460	ND1.3 + ND0.4	ND0.6	2,860
	ND2.0	ND0.6	5,800	ND2.0	ND0.6	4,600

Interpretation summary. The KRISS-assigned, model-specific MOR values are retained as calibration inputs. Their independent revalidation is outside this study. In the effective-extinction model, $V_{cal,i} = V_{r,i}$. Acceptance of the reference assignment does not itself validate additive background extinction.

Manuscript Table 3

Table 3: Log-domain regression statistics for indoor darkroom and outdoor filter tests. Slopes and intercepts are reported as estimate ± standard error. $CI_{a_{ln}}$ and CI_C denote approximate 95% confidence-interval half-widths, calculated using Student-t multipliers and first-order propagation of the covariance from the inverse log-domain regressions. Each PWD22 regression contains six filter points, and each SWS-200 regression contains five. These intervals describe conditional regression uncertainty and do not constitute a complete calibration uncertainty budget. Point CV denotes the mean pointwise coefficient of variation derived from the 1 min observations.

Environment	Instrument	Filter set	Sequence	Slope (a_{ln})	$CI_{a_{ln}}$ (95 %)	Intercept (C)	CI_C (95 %)	R^2	Point CV (%)
Indoor	PWD22_A01	B	1	0.993 ± 0.005	0.014	-0.007 ± 0.034	0.094	1.000	0.546
		B	2	0.992 ± 0.005	0.014	0.005 ± 0.035	0.097	1.000	0.643
		E	1	0.965 ± 0.018	0.050	0.147 ± 0.127	0.352	0.999	0.472
		E	2	0.964 ± 0.013	0.037	0.146 ± 0.093	0.259	0.999	0.546
	PWD22_B01	B	1	0.996 ± 0.002	0.005	-0.024 ± 0.013	0.035	1.000	0.796
		B	2	1.001 ± 0.004	0.011	-0.068 ± 0.029	0.079	1.000	0.478
		E	1	0.996 ± 0.005	0.014	-0.074 ± 0.037	0.102	1.000	0.703
		E	2	0.997 ± 0.005	0.015	-0.075 ± 0.039	0.107	1.000	0.711
	SWS-200_B03	B	1	0.998 ± 0.023	0.075	-0.057 ± 0.172	0.546	0.998	0.221
		B	2	0.999 ± 0.024	0.075	-0.064 ± 0.173	0.551	0.998	0.297
		E	1	1.113 ± 0.045	0.143	-0.804 ± 0.325	1.034	0.995	0.224
		E	2	0.982 ± 0.021	0.067	0.163 ± 0.151	0.480	0.999	0.267
Outdoor	PWD22_B01	B	1	0.969 ± 0.013	0.035	0.125 ± 0.088	0.243	0.999	1.174
		E	1	0.974 ± 0.016	0.045	0.097 ± 0.114	0.316	0.999	1.637
	SWS-200_B03	B	1	0.995 ± 0.014	0.043	0.017 ± 0.099	0.315	0.999	0.220
		E	1	1.003 ± 0.009	0.030	0.033 ± 0.068	0.216	1.000	0.258

Interpretation summary. Point estimates are unchanged. Standard errors and approximate 95 % interval half-widths were recalculated under the stated inverse-OLS convention, including covariance propagation. Each PWD22 fit uses six filter points and each SWS-200 fit five. Point CV describes within-interval variability; it is neither regression uncertainty nor remounting reproducibility. All PWD22 darkroom slope intervals include unity.

Manuscript Table 4

Table 4: Adopted darkroom and outdoor regression intercepts and the corresponding empirical factors $f_{\mathrm{env,reg}} = \exp(C_{\mathrm{out}} - C_{\mathrm{dark}})$. The logarithmic intercept contrast is defined as $\Delta C = C_{out} - C_{dark}$. Approximate 95 % confidence intervals for ΔC combine the propagated uncertainties of the adopted indoor and outdoor intercepts, assuming independent fitted random errors. Confidence intervals for $f_{\mathrm{env,reg}} = exp(\Delta C)$ are obtained by exponentiating the corresponding interval endpoints. These conditional intervals treat reference values as fixed and exclude shared reference uncertainty and other systematic contributions. The PWD22 factors are calculated from B01 darkroom and outdoor regressions. SWS-200 Set E uses darkroom Sequence 2 and outdoor Sequence 1. The factors describe fitted intercept differences and are not automatically equivalent to physical outdoor/darkroom MOR ratios.

Sensor unit	Filter set	Darkroom seq.	Outdoor seq.	C_{dark}	C_{out}	ΔC	Approx. 95 % CI for ΔC	$f_{env,reg}$	Approx. 95 % CI for factor	LT31 MOR (mean ± SD)
PWD22 B01	B	1	1	-0.024	0.125	0.149	−0.093 to 0.391	1.161	0.912 to 1.478	14,997 ± 47 m
	E	1	1	-0.074	0.097	0.171	−0.139 to 0.481	1.187	0.870 to 1.618	14,777 ± 717 m
SWS-200 B03	B	1	1	-0.057	0.017	0.074	−0.441 to 0.590	1.077	0.643 to 1.804	10,740 ± 2,797 m
	E	2	1	0.163	0.033	-0.130	−0.582 to 0.322	0.878	0.559 to 1.380	15,000 ± 0 m

Interpretation summary. All four ΔC intervals include zero at $V_* = 1\ m$, and all factor intervals include unity. This does not establish that the fitted responses are equal throughout the measured range. The negative SWS-200 Set-E contrast is retained. LT31 means and sample SDs pool the available one-minute readings within the selected KST filter intervals, excluding gaps. Ceiling-censored values establish neither the true background nor its constancy.

Manuscript Table 5

Table 5: Long-term field validation performance summary (17 Aug 2023 – Feb 2024).

Metric	PWD22 A01			SWS-200 B03		
	Raw	Set B	Set E	Raw	Set B	Set E
Valid pairs (n)	33,152			32,018		
Pearson r	0.843			0.820		
OLS slope (log-space)	0.90	0.90	0.93	0.94	0.94	0.94
Log-bias (μ, log_{10})	−0.010	+0.020	+0.062	+0.030	+0.042	+0.004
Log-RMSE (δ, log_{10})	0.190	0.192	0.204	0.217	0.220	0.215
Within ±10 % benchmark	17.9 %	24.5 %	39.2 %	35.0 %	27.9 %	42.8 %

Interpretation summary. These results assess selected regression corrections. A01 Set E improves the benchmark agreement fraction but increases absolute bias and RMSE. B03 Set E improves these metrics; B03 Set B does not. The uniform ±10 % benchmark is not a WMO-compliance assessment. Pearson r is unchanged because positive affine transformations in log space preserve it; slopes can change even when rounding hides that change.

A5 Table 5 reproduction

The reproduction paired the organised A01, B03 and LT31 input series by timestamp from 17 August 2023 through February 2024, on the confirmed KST time basis. No additional smoothing was applied. Values were excluded where A01 equalled 7,999 m or exceeded 19,500 m, where B03 was at 20,000 m, and where LT31 exceeded 14,000 m; each pair also required positive, non-missing values. The retained counts are 33,152 for A01 and 32,018 for B03.

The calculation retains the coefficients actually used in the historical scripts, listed in the response to Comment 2. Substituting unrounded coefficients would be a different numerical calculation, not a reproduction. The reproduced counts, Pearson correlations, OLS slopes, log-biases, log-RMSEs and revised benchmark fractions agree with Table 5 at its displayed precision.

Calibration uses natural logarithms, whereas performance evaluation uses base-10 residuals. Each residual is log_{10} (sensor MOR/LT31 MOR); global log-bias is their arithmetic mean, and log-RMSE is the square root of their mean squared value. The benchmark fraction counts ratios from 0.90 to 1.10, inclusive. The revised fractions therefore replace the original log-symmetric bounds, while the corrected MOR series and the bias and RMSE results are unchanged.

These results were reproduced from the organised analysis files. The reproduction is not an independent audit of every upstream raw-data processing step, and the field comparison does not independently validate physical environmental decoupling.

A6 Summary of figure changes relevant to RC1

Figure 2 retains the multiplicative-error illustration without presenting a universal ±10 % band as a WMO requirement. Figure 3 distinguishes the empirical intercept difference from its conditional physical interpretation. Figure 5 uses the recalculated approximate 95 % coefficient-interval half-widths; point error bars describe within-interval standard deviations.

Figure 6 now contains model curves only, for illustrative indoor backgrounds of 20,000 m, 50,000 m and negligible indoor background extinction, with filter-equivalent MOR values of 220, 1,000, 5,000, 10,000 and 15,000 m. The previous event markers and grey crosses have been removed. These scenarios are neither estimates of the laboratory background nor fits to the intercept factors.

Figures 8 and 9 retain the reproduced correction results and use benchmark boundaries at $log_{10}(0.90)$ and $log_{10}(1.10)$, with revised fractions consistent with Table 5. Their interpretation distinguishes bias, residual scatter and benchmark agreement rather than claiming universal improvement or physical separation.